Measurement of the energy dependence of the $e^+e^- \to B\bar{B}, B\bar{B}^*$, and $B^*\bar{B}^*$ cross sections at Belle II

Sergey Privalov

Budker Institute of Nuclear Physics of SB RAS, Novosibirsk

The 7th International Conference on Particle Physics and Astrophysics,
22-25 October 2024, Moscow

Motivation

Dong,Mo,Wang,Yuan CPC**44**, 083001 (2020)

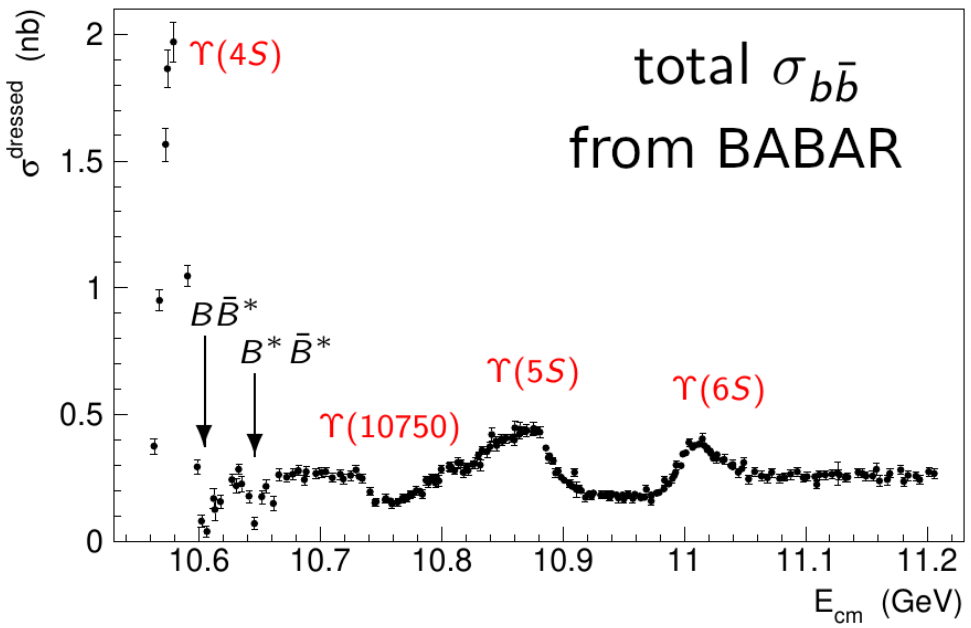

Ono,Sanda,Tornqvist PRD**34**,186(1986)

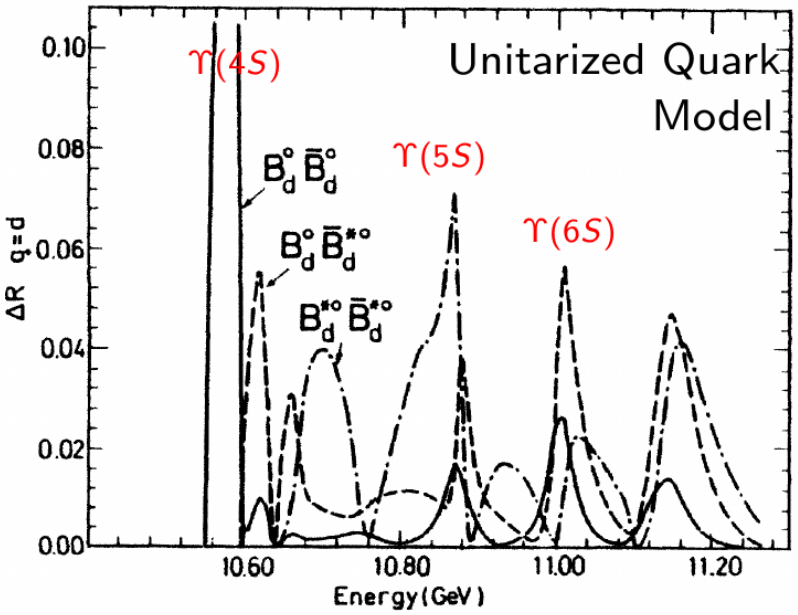

Total $e^+e^- \to b\bar{b}$: peaks of $\Upsilon(4S)$, $\Upsilon(5S)$, and $\Upsilon(6S)$, dips at $B\bar{B}^*$ and $B^*\bar{B}^*$ thresholds and at $\Upsilon(10750)$.

Exclusive cross sections are expected to have more structures. Unitarized Quark Model: minima are due to nodes of the $\Upsilon(4S, 5S, 6S)$ wave functions – information about Υ states.

Belle measurement: [R. Mizuk *et al.* [Belle Collaboration], JHEP **06**, 137 (2021)]: oscillatory behavior of exclusive cross sections.

Experimental setup

The SuperKEKB accelerator

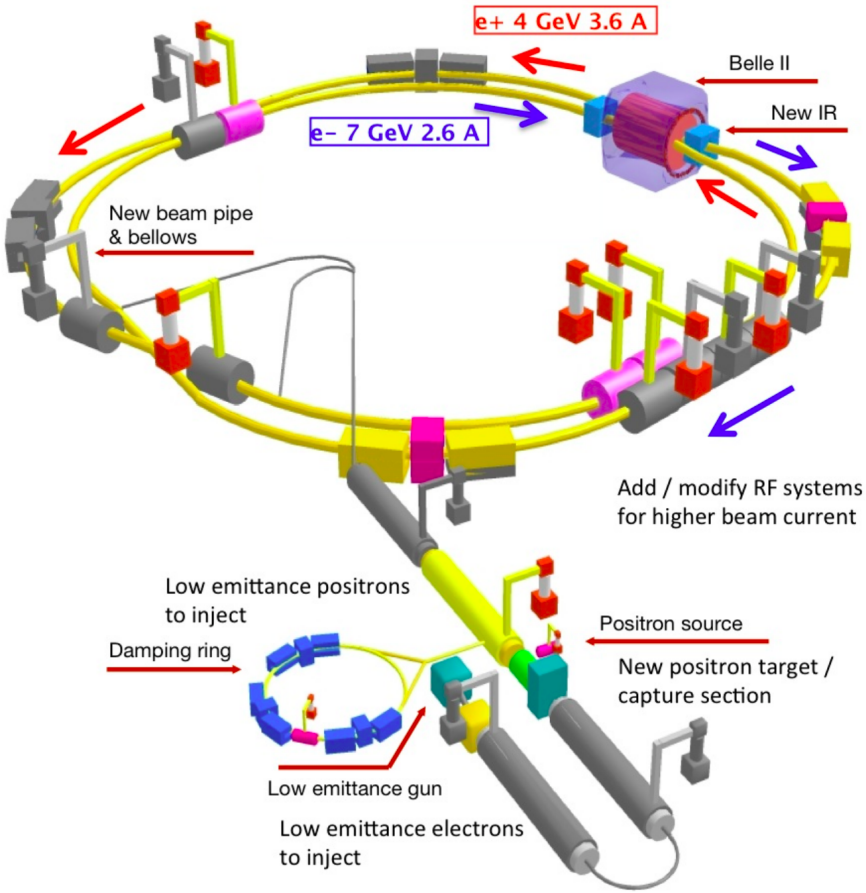

B-factory with luminosity $\mathcal{L} = 4.71 \cdot 10^{34}\ \mathrm{cm}^{-2}\mathrm{s}^{-1}$.

The Belle II detector

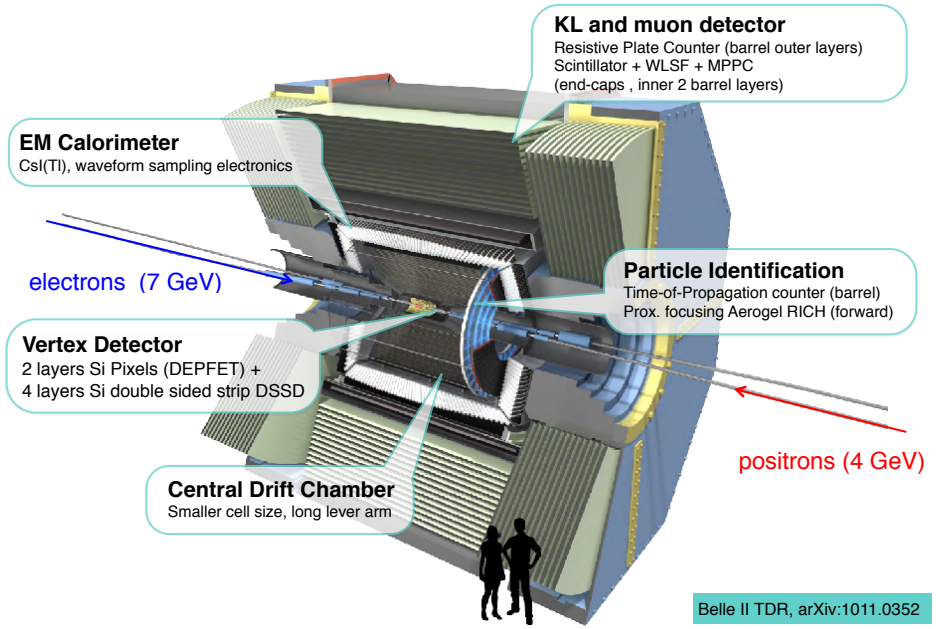

General purpose spectrometer that efficiently collects data of e^+e^- collisions.

Overview of the analysis

Data samples:

E_{cm}, MeV	$\Upsilon(4S)$	10653	10701	10746	10805
L, fb^{-1}	35.5	3.5	1.6	9.8	4.7

Reconstruct B mesons in a large number of hadronic final states (≥ 1000). Use automated procedure from Belle II software that includes machine learning for selection. Advantage: higher flexibility.

Identify $e^+e^- \to B\bar{B}$, $B\bar{B}^*$ and $B^*\bar{B}^*$ using $M_{\text{bc}} = \sqrt{(E_{\text{cm}}/2)^2 - p_B^2}$, p_B — B meson momentum. Photons from $B^* \to B\gamma$ are not reconstructed $\Rightarrow$ in $\Delta E = E_B - E_{\text{cm}}/2$ the $B^*\bar{B}^{(*)}$ signals are shifted. Rotation: $\Delta E' = \Delta E + M_{\text{bc}} - m_B$; all signals peak at zero and have the same shape. Use $\Delta E'$ sidebands to constrain background.

Event selection

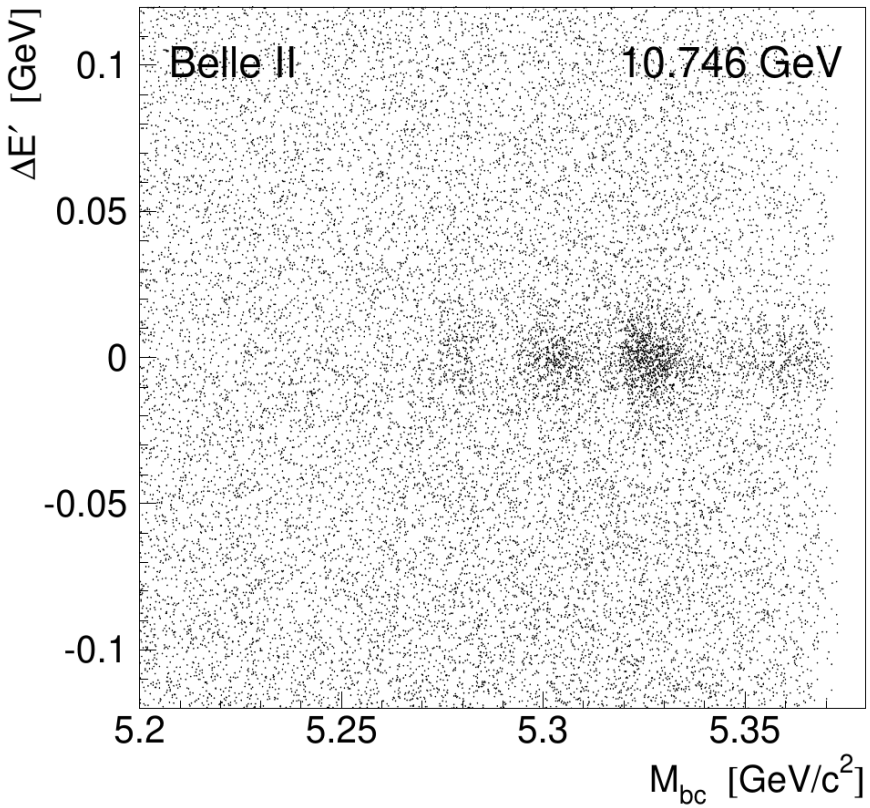

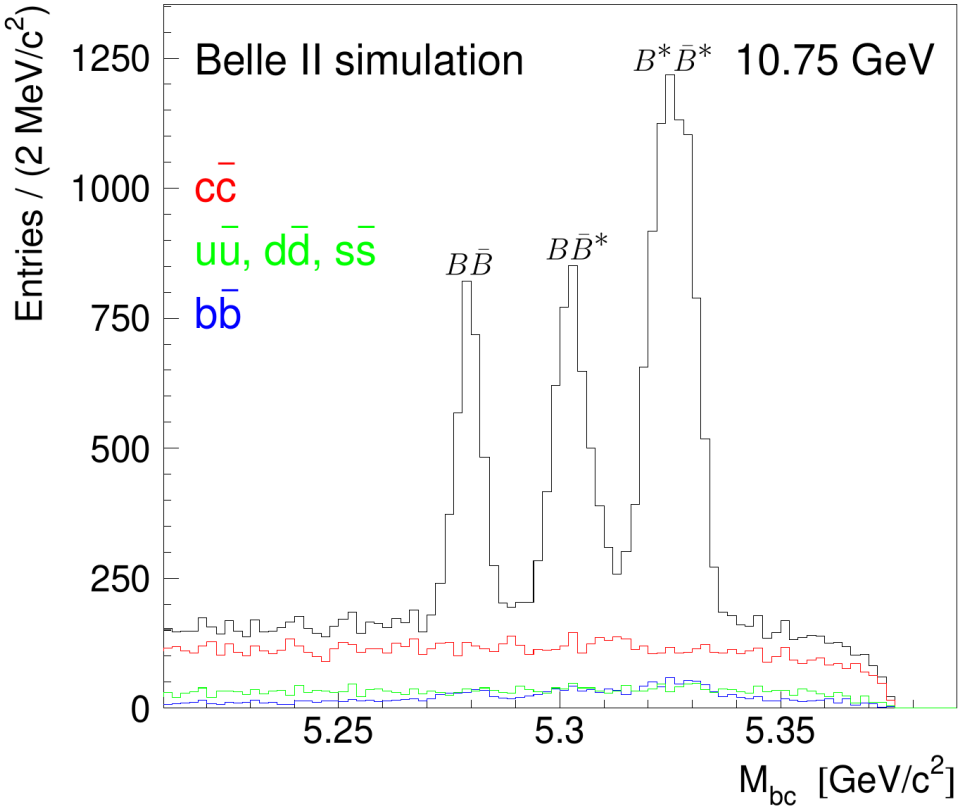

Choose MVA input variables that are not correlated with p_B. Monte-Carlo (MC) simulation is used to optimize the selection criteria for variables $|\Delta E'|$ and MVA output. Obtained ratio between efficiencies: $\frac{\varepsilon[\Upsilon(5S)]}{\varepsilon[\Upsilon(4S)]} = 1.032 \pm 0.012$.

Data and simulation show prominent signals after selection.

M_{bc} fit function

Example at $\Upsilon(5S)$:

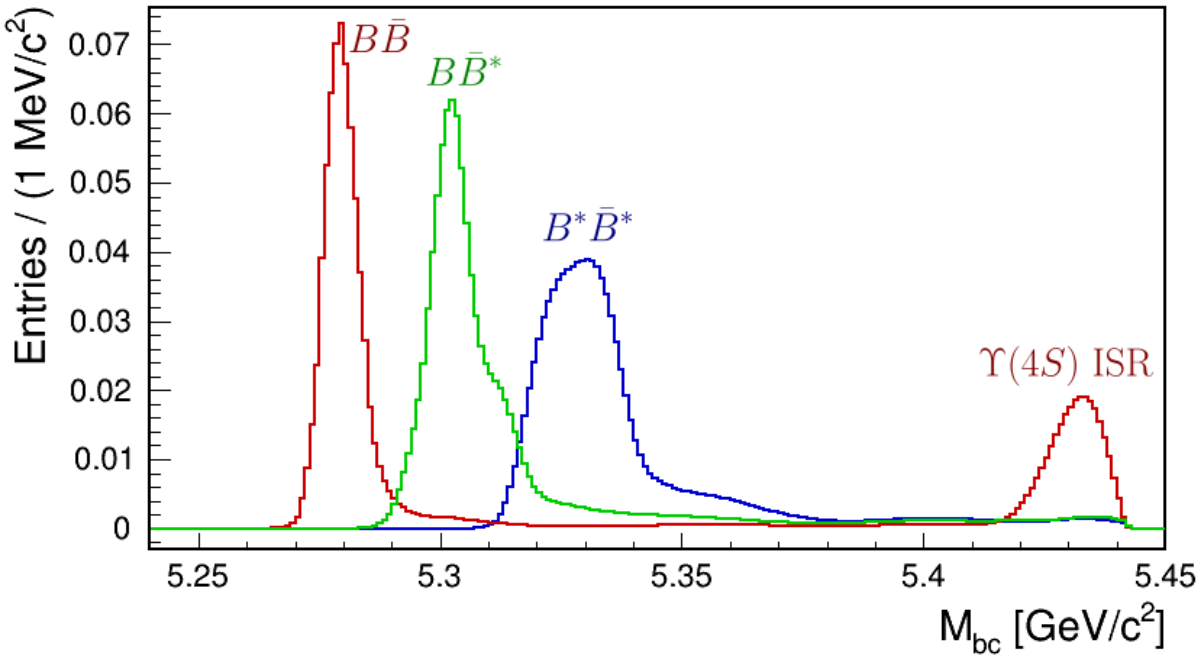

Fit function is calculated numerically and takes into account: E_{cm} spread, energy dependence of cross section, initial state radiation (ISR), momentum resolution, peaking background, and kinematics of $B^* \to B\gamma$.

$B^* \to B\gamma$: distribution in helicity angle is $1 + a_h \cos^2\theta$.
For $B\bar{B}^*$ expect $a_h = 1$, for $B^*\bar{B}^*$ a_h is not fixed.

Fit of M_{bc} in $\Upsilon(4S)$ simulation

Selected events of MC simulation are divided into three categories:

- true signal:
  $|\Delta E'| < 18$ MeV,
  pass truth-matching;
- broken signal:
  $|\Delta E'| < 18$ MeV,
  fail truth-mathing;
- $\Delta E'$ sideband:
  $|\Delta E' - 80 \text{ MeV}| < 18$ MeV.

Parameters of the momentum resolutions and ratios between event categories are obtained.

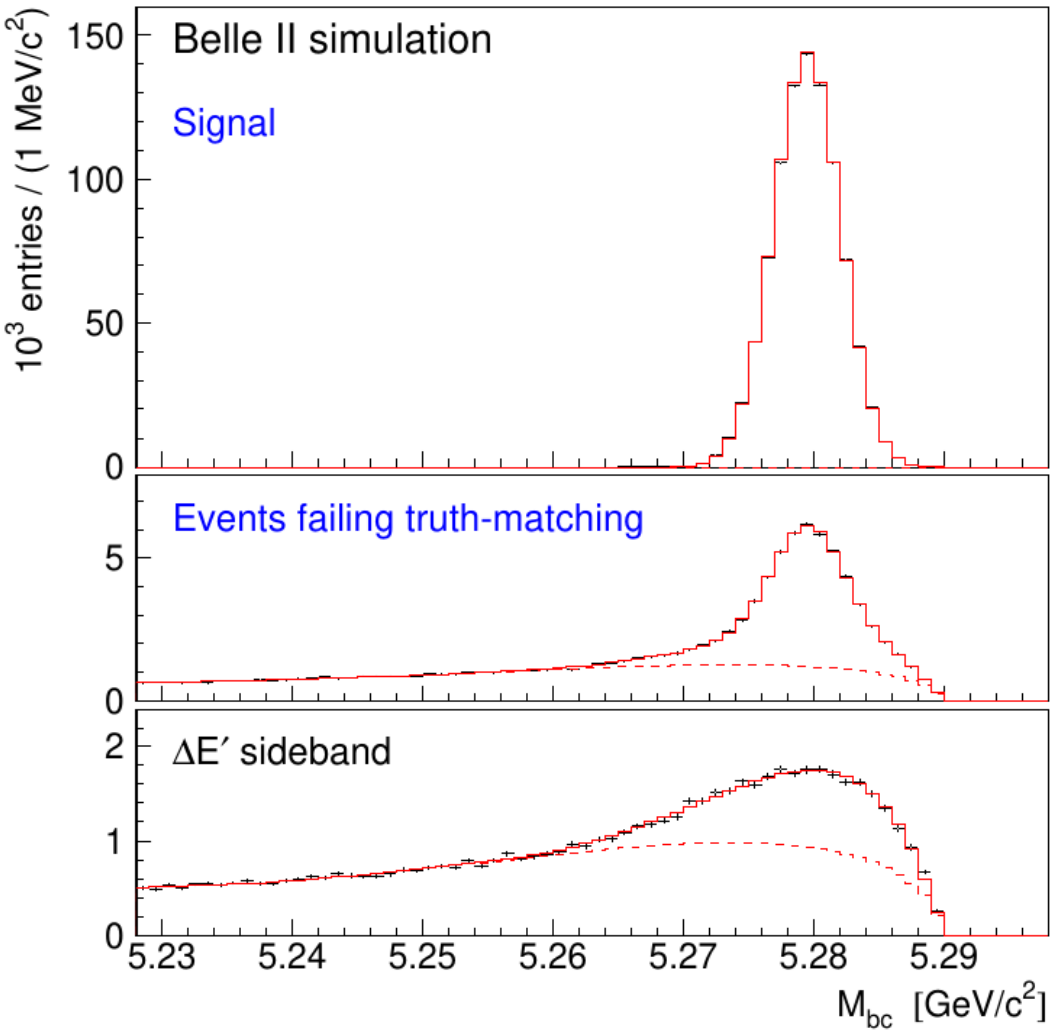

Determination of the efficiency of B reconstruction at $\Upsilon(4S)$

Simultaneous M_{bc} and cross section fit

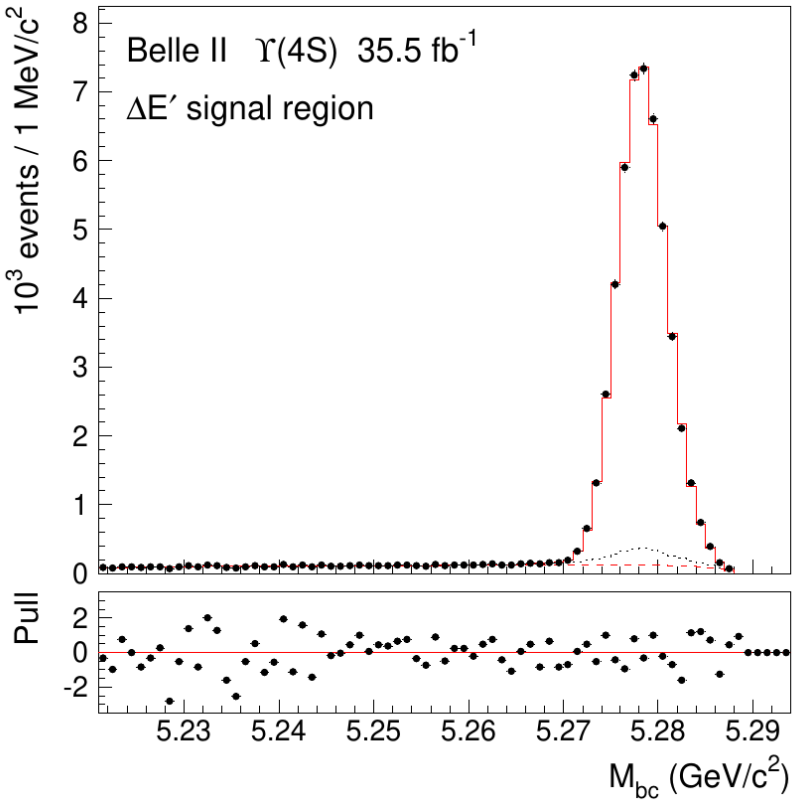

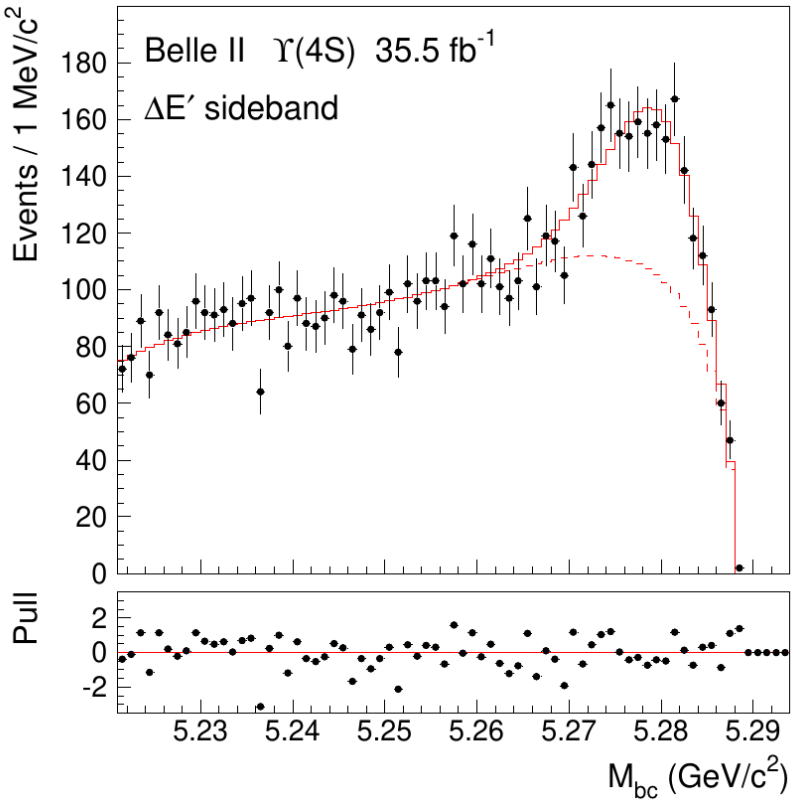

$$\epsilon = \frac{N}{2N_{B\bar{B}}} = (0.5892 \pm 0.0031 \pm 0.0116) \times 10^{-3},$$

$N_{B\bar{B}}$ — total number of $B\bar{B}$ events, measured using the difference between multihadronic events at the $\Upsilon(4S)$ peak and below the $B\bar{B}$ threshold.

M_{bc} fits in scan data

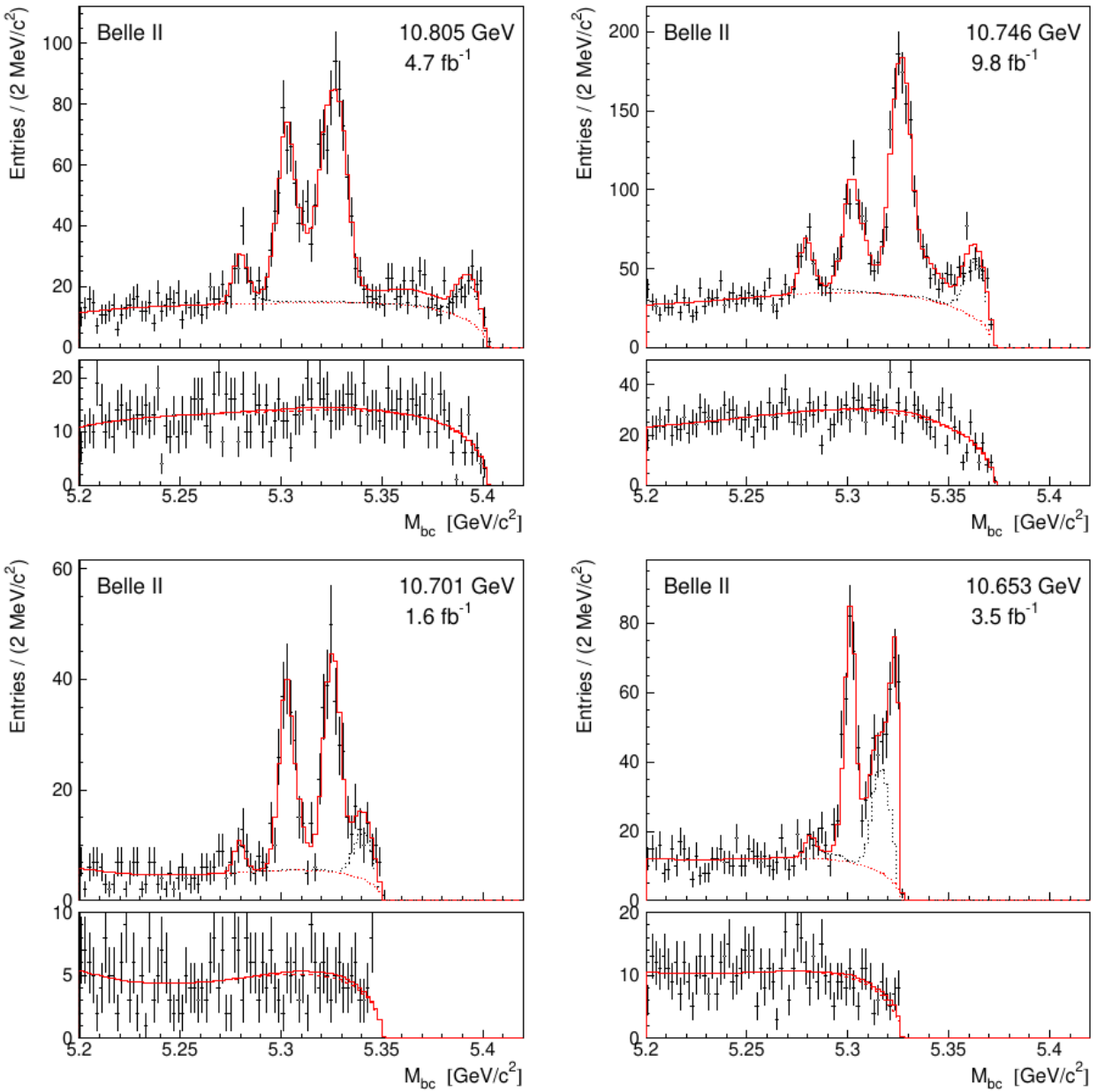

Results

Dressed cross sections are calculated iteratively in sequential simultaneous fits of cross sections' energy dependencies and M_{bc} distributions:

$$\sigma_{\mathrm{dressed}}^{(\text{this iteration})} = \frac{N}{L\varepsilon(1+\delta_{\mathrm{ISR}})^{(\text{previous iteration})}},$$

N — number of signal events, ε — linearly changing efficiency,
L — integral luminosity, $1+\delta_{\mathrm{ISR}}$ — radiative correction.

point#	$\sigma(e^+e^- \to B\bar{B})$ (pb)	$\sigma(e^+e^- \to B\bar{B}^*)$ (pb)	$\sigma(e^+e^- \to B^*\bar{B}^*)$ (pb)
1	$21.0 \pm 4.1 \pm 0.5 \pm 0.5$	$98.6 \pm 6.8 \pm 1.3 \pm 2.3$	$143.6 \pm 8.4 \pm 2.4 \pm 3.3$
2	$19.0 \pm 2.9 \pm 1.0 \pm 0.4$	$52.9 \pm 4.2 \pm 1.0 \pm 1.2$	$104.0 \pm 4.8 \pm 2.7 \pm 2.4$
3	$16.1 \pm 6.0 \pm 0.7 \pm 0.4$	$126.0 \pm 11.8 \pm 2.2 \pm 2.8$	$151.4 \pm 13.4 \pm 2.8 \pm 3.4$
4	$7.2 \pm 3.3 \pm 1.4 \pm 0.2$	$106.8 \pm 7.8 \pm 3.7 \pm 2.3$	$64.5 \pm 6.4 \pm 2.7 \pm 1.4$

Table: dressed cross sections. The first error is statistical, the second is uncorrelated systematic and the third is correlated systematic. Points are in the descending energy order.

Cross sections energy dependence

R_b^{dressed} and Belle measurements are used to constrain the fits.
Rapid rise of $B^*\bar{B}^*$ dressed cross section is observed.

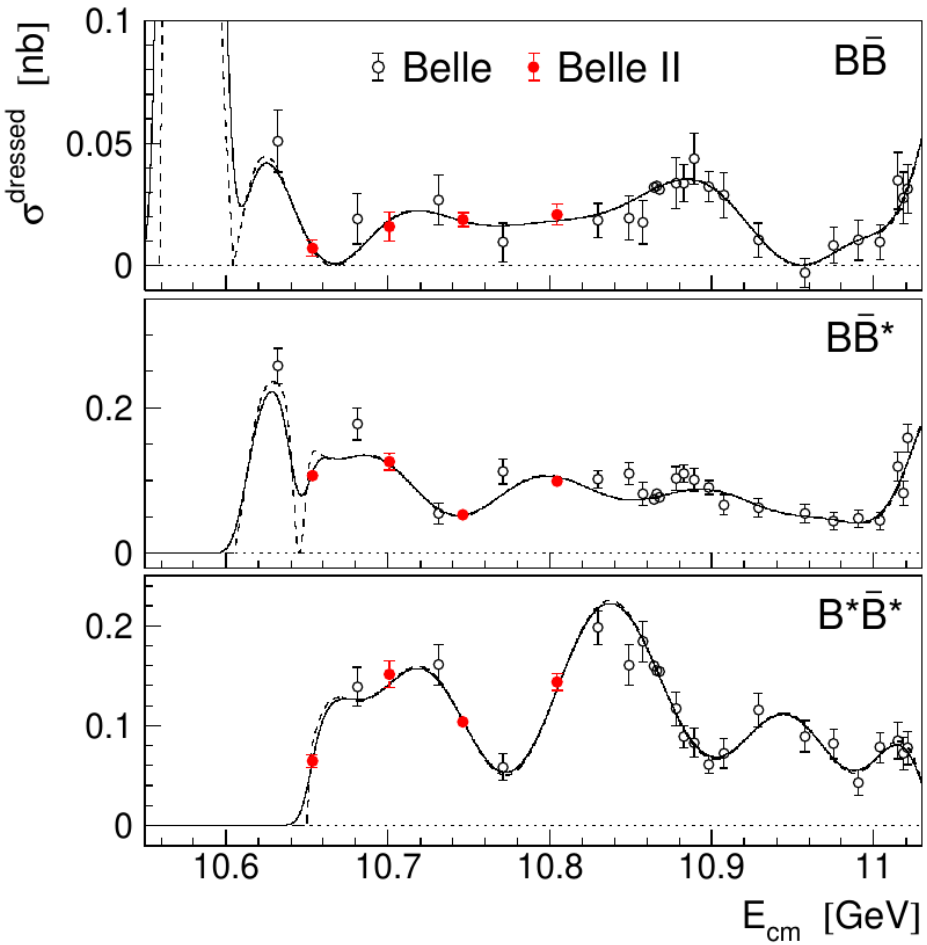

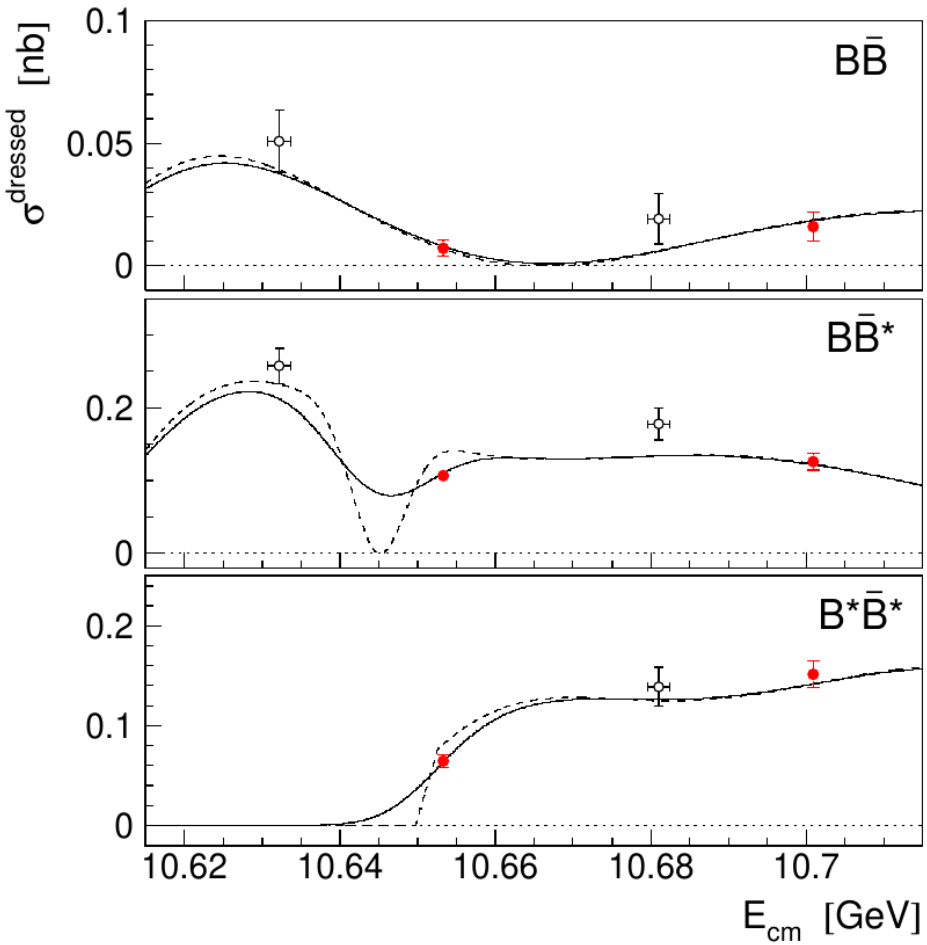

Discussion

Phenomenological analysis [Nucl. Phys. A **1041**, 122764, (2024)]:

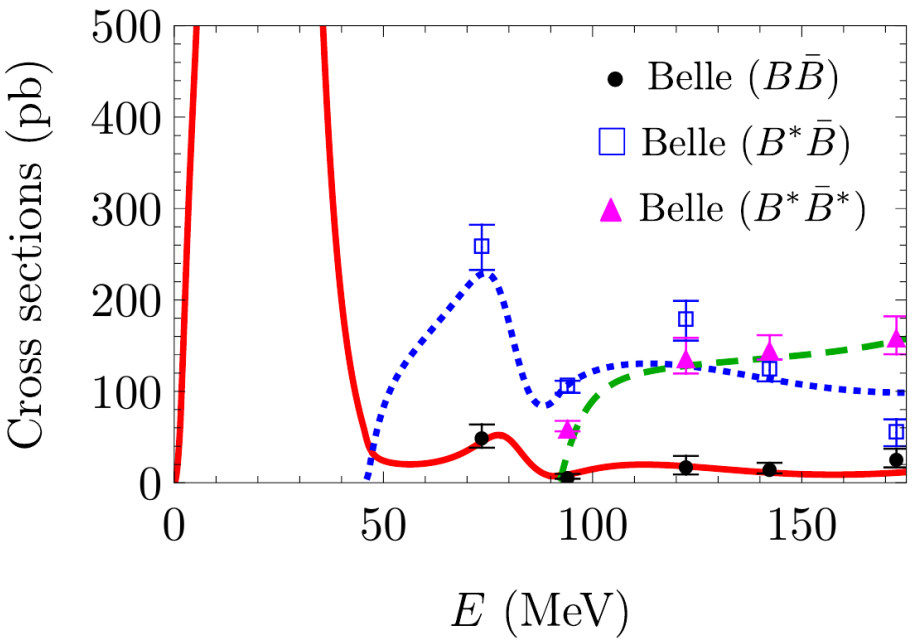

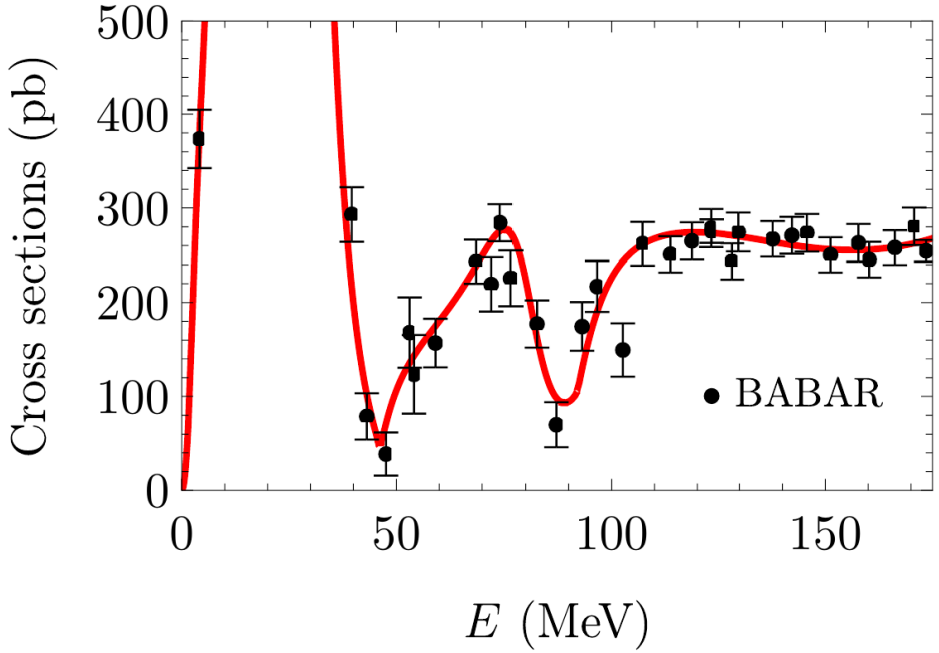

- Non-trivial shape of the cross sections is the result of the transitions between different channels: $B\bar{B}, B\bar{B}^*$, and $B^*\bar{B}^*$.
- Bound state of $B^*\bar{B}^*$ 25 MeV below the corresponding threshold.

Conclusion

Exclusive cross sections of $e^+e^- \to B\bar{B}, B\bar{B}^*, B^*\bar{B}^*$ were measured at 4 energies between 10.65 and 10.80 GeV with total integrated luminosity of 19.7 fb^{-1} at Belle II. The cross section $e^+e^- \to B^*\bar{B}^*$ increases very rapidly near the corresponding threshold (possible $B^*\bar{B}^*$ molecular state).

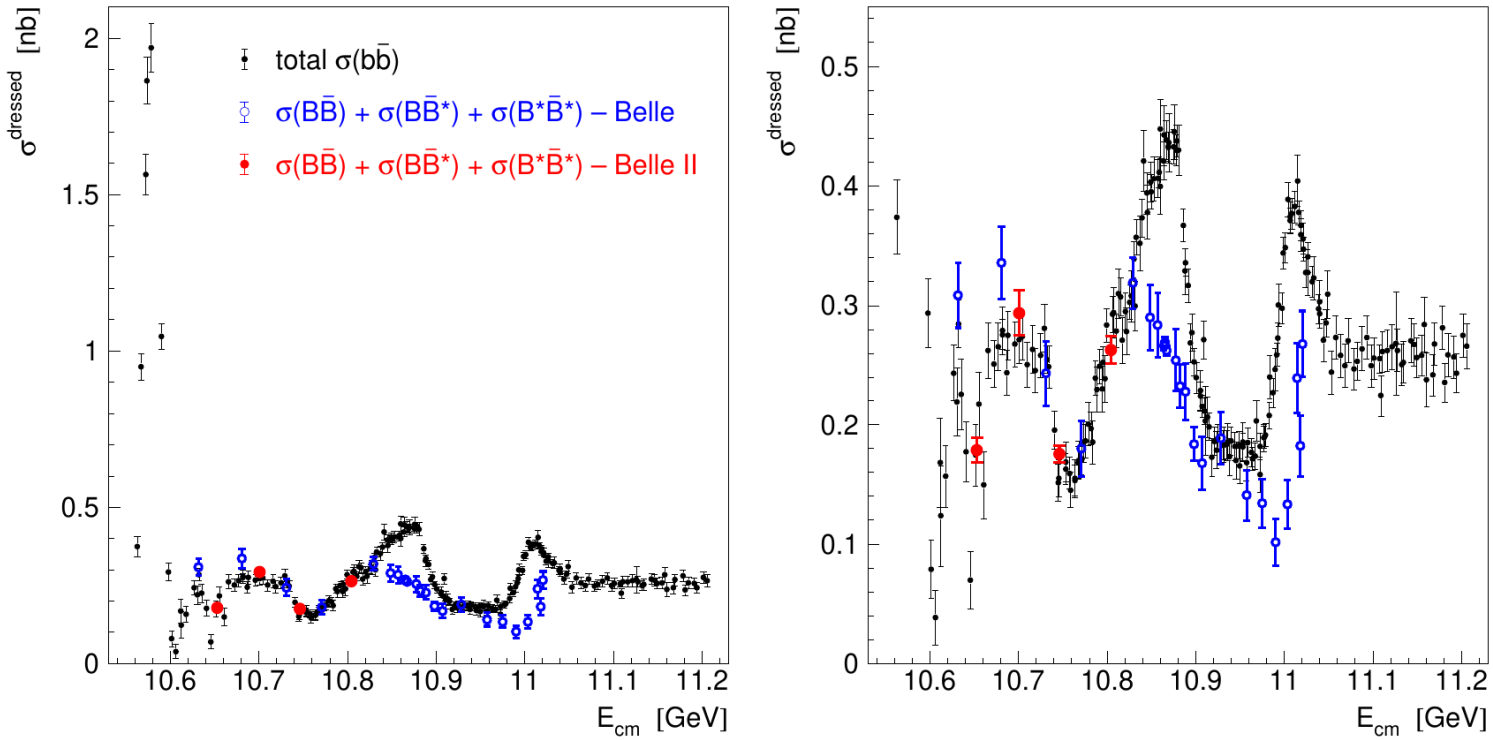

Results are consistent with the Belle measurement.
Preprint [arXiv:2405.18928v2 [hep-ex]], accepted by JHEP.